G. Lacalle, I. Val, Ó. Seijo, M. Mendicute, D. Cavalcanti and J. Perez - Ramirez, "Multi-AP Coordination PHY/MAC Management for Industrial Wi-Fi," 2022 IEEE 27th International Conference on Emerging Technologies and Factory Automation (ETFA), Stuttgart, Germany, 2022, pp. 1-8.

DOI: https://doi.org/10.1109/ETFA52439.2022.9921700

Multi-AP Coordination PHY/MAC Management for Industrial Wi-Fi

Guillermo Lacalle[1], Iñaki Val[1], Óscar Seijo[1], Mikel Mendicute[2], Dave Cavalcanti[3] and Javier Perez – Ramirez[3]
[1]Ikerlan Technology Research Centre, Basque Research and Technology Alliance (BRTA), Mondragón, Spain
[2]Mondragon Unibertsitatea, Mondragón, Spain
[3]Intel Corporation, USA

Abstract— **This work discusses Access Point Coordination techniques for future 802.11 communications in the context of industrial Wireless TSN scenarios. A Coordinated OFDMA setup is proposed with a frame exchange scheme based on implicit wireless channel sounding prior to transmission. The scheduler assigns resource units to the users, trying to maximize the probability of all the STAs in the network to successfully deliver their data. In order to evaluate the quality of the channels without introducing overhead in the network, we propose a virtual sounding mechanism. We present simulation results first to validate the virtual sounding mechanism and, second, to show the achievable reliability of a Multi-AP network for a set of representative scenarios. These results highlight that Multi-AP can be effectively used to enhance the reliability of the network though special attention must be taken for time-varying scenarios.**

Key Terms — Industry 4.0, Factory Automation, TSN, Wireless TSN, Wi-Fi, AP Coordination, C-OFDMA.

I. INTRODUCTION

Industry factory floors and process automation environments require reliable, secure, and efficient communications. Therefore, wired communications are typically used in such scenarios. Nowadays, Ethernet is considered the main technology for future wired industrial networks, in particular, when combined with Time-Sensitive Networking (TSN) [1]. TSN is a set of sub-standards compiled in IEEE 802.1, designed to allow reliable, deterministic, and low jitter communications over wired networks.

With the arrival of different fields of study in the so-called industry 4.0 [2], like Robotics and the Internet of Things (IoT) [3][4], wires manifest evident limitations in terms of flexibility, scalability, and deployment costs. Wireless communications have been recently considered as a suitable alternative to wired, resulting in a strong research trend around porting the TSN technology into wireless (WTSN) [5]. Despite this strong interest, the development of a WTSN technology that offers similar capabilities as the wired TSN is quite challenging. These challenges come, in the first place, from the Quality of Service (QoS) required in many real-time applications [6] including low Packet Error Rate (PER), and low deterministic latency, and in the second place, from the inherent issues of wireless communications such as multipath propagation, fading, and interference.

The WTSN research trend has led to the emergence of new techniques that have been adopted by the most advanced wireless standards, such as IEEE 802.11 and 3GPP 5G [7][8]. These technologies have made great strides in the direction of more efficient and controlled networks and have laid the groundwork for future modifications to further enhance the capabilities of the wireless technologies and reach the performance targets expected by the industry [9].

Regarding 5G, these networks are considered as one of the wireless options to support the industry requirements thanks to the Ultra-Reliable Low Latency Communications (URLLC) profile. 3GPP Release 16 defines the functionalities to integrate 5G within a TSN network at a logical level thanks to a TSN translator that interconnects nodes between both networks [8].

Regarding IEEE 802.11, it works in unlicensed bands and, despite the novel inclusion of the 6 GHz band, this translates into possible interferences between devices, which can even use different protocols such as Bluetooth. To enable a more controlled scenario within the 802.11 protocol, the last standard 802.11ax has included PHY/MAC mechanisms such as Orthogonal Frequency Division Multiple Access (OFDMA) and a Trigger Frame (TF) [10], which are depicted in Fig 1. However, these features are comprised within a single Basic Set Service (BSS) and no interference between adjacent BSS relies on transmission power thresholds and different frequency operations.

With the upcoming release of the new 802.11be standard, further techniques are meant to be included such as Multi-Link Operation, which has been demonstrated by simulations to improve the reliability and latency of the communication [11]. In addition, other proposed technologies such as Multi Access Point (AP) Coordination are expected to be included in future releases after 802.11be [12]. However, to the best of our knowledge, the state-of-the-art focuses on single AP networks with no coordination between APs [13] and there is no available study showing the capabilities of IEEE 802.11 Multi-AP Coordination for industrial applications.

Multi-AP Coordination compiles different techniques that can be configured to obtain a more reliable, interference-free, and deterministic access to the medium. However, Multi-AP Coordination is a complex technique that relies on having good knowledge of the quality of the link to operate [14]. Multi-AP Coordination must be therefore always combined with channel sounding techniques, which may increase the overhead network. Thus, appropriate network design and scheduling are vital to properly use Multi-AP Coordination.

Distributed MIMO or Joint Transmission (JTx) schemes have been proposed in [15], dividing the transmission into slots to provide fairness constraints, but not exploiting the OFDMA frequency flexibility. In [16], the authors take advantage of OFDMA for scheduling user resources proposing a proprietary MAC protocol. Nevertheless, this work is not focused on Multi-AP Coordination. A transmission scheme for Coordinated OFDMA (C-OFDMA)

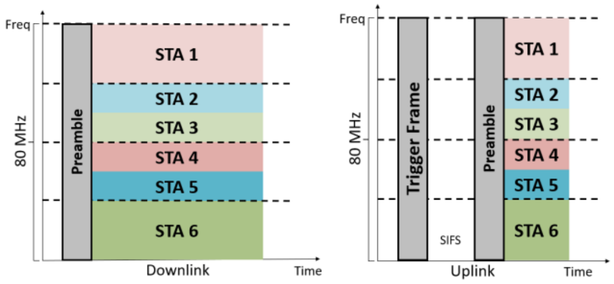

Figure 1. OFDMA resources allocation in Downlink and Uplink.

has been proposed in [17], which improves the system throughput by allowing an AP to share a granted transmission opportunity (TXOP) with nearby APs. However, this study does not focus on the frequency diversity provided by the combination of OFDMA and Multi-AP Coordination. In summary, none of the previous papers study the Multi-AP Coordination from an OFDMA allocation perspective. By the other hand and to the best of our knowledge, every OFDMA scheduler proposals in the literature are based on STA's size queues and the Buffer Status Request/Report (BSR) mechanism. Whereas we propose a scheduler that attempts to maximize the probability of every STA to successfully communicate its data.

This paper presents an analysis of the potential benefits in terms of PER that the IEEE 802.11 Multi-AP Coordination can provide in the context of WTSN Operation. We first present the techniques that have been proposed for future 802.11 standard releases and we focus our analysis on one of them: C-OFDMA. We propose the use of a channel sounding scheme and a scheduler algorithm to perform the allocation of the user's data in the C-OFDMA network. We present a simulation setup to evaluate the proposed scheme under realistic wireless conditions. The results obtained by numerical simulation show that C-OFDMA can significantly improve the reliability of the network, especially under low time-varying wireless channels.

The rest of the paper is organized as follows. Section II provides a background of the concepts and technologies involved in this article. Section III describes our proposed C-OFDMA scheduler algorithm and channel sounding mechanisms used to evaluate the channel quality. Section IV presents the wireless network simulation setup. In Section V we II. show and discuss our numerical simulation results. Finally, section VI concludes the article and introduces future research directions.

CURRENT STATE AND FUTURE OF 802.11 FOR INDUSTRIAL APPLICATIONS

This Section presents the main features of current IEEE 802.11 and discusses the Multi-AP Coordination techniques that are being proposed for next generation IEEE 802.11.

A. Trigger Frame and Multi-User OFDMA Operation

Despite being a well-known medium access technique used in standards such as Long-Term Evolution (LTE), OFDMA alongside the TF were introduced in Wi-Fi with the 802.11ax amendment [10]. Since then, Wi-Fi devices have now the option to use OFDMA Multi-User transmission by allocating its information into specified Resource Units (RUs). These

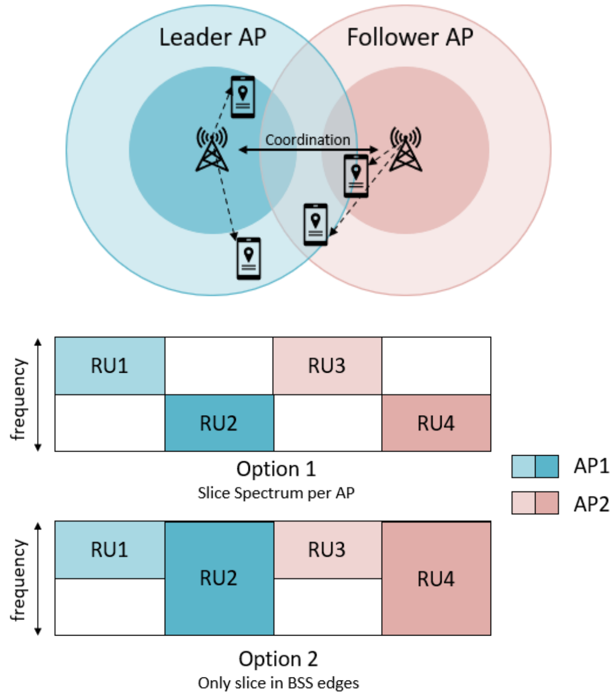

Figure 2. Coordinated OFDMA, frequency resources are restricted for nearby APs so they can transmit simultaneously with no interference [19].

RUs are made up of sets of subcarriers within an OFDMA frame that
are assigned to specific users. Figure 2 represents the slicing of the bandwidth resources to different Stations (STAs).

The exact allocation and bandwidth for each RU depend on the number of devices that the Access Point (AP) schedules in a specific transmission. The OFDMA Downlink (DL) transmissions are directly performed by the AP indicating the RU allocation in the PHY header of the DL Multi User (MU) frame. The STAs use the header to know which slot is assigned to which STA. On the other hand, the RUs for Uplink (UL) transmissions are also assigned by the AP. To this end, the AP transmits a TF which includes the RU allocation of each STA. The STAs then use the TF to timely coordinate their OFDMA transmission and to know which resources of the OFDMA grid are assigned to each STA. To know which STAs have data to transmit, the standard defines the BSR . The BSR is used by the APs to poll the STAs to know the number of bytes waiting in their transmission buffers.

Even though OFDMA and the TF allow scheduled operations over 802.11, the transmissions are still based on non-deterministic Medium Access Control (MAC), using a Carrier-Sense Multiple Access with Collision Avoidance (CSMA/CA)
which means that any device that wants to transmit is forced to listen to the channel for a period of time to check if the channel is free or not. If the data frames are lost, retransmissions are required, which drastically impacts the latency of the communication [10]. Therefore, using as few retransmissions as possible (i.e., by having a low PER), leads to a significant reduction of the mean and worst-case communication latency [11]. However, reaching a low PER is quite challenging in wireless environments, due to the possibility of interference from nearby networks, and common propagation phenomena. To address this issue, we show that Multi-AP Coordination combined with OFDMA

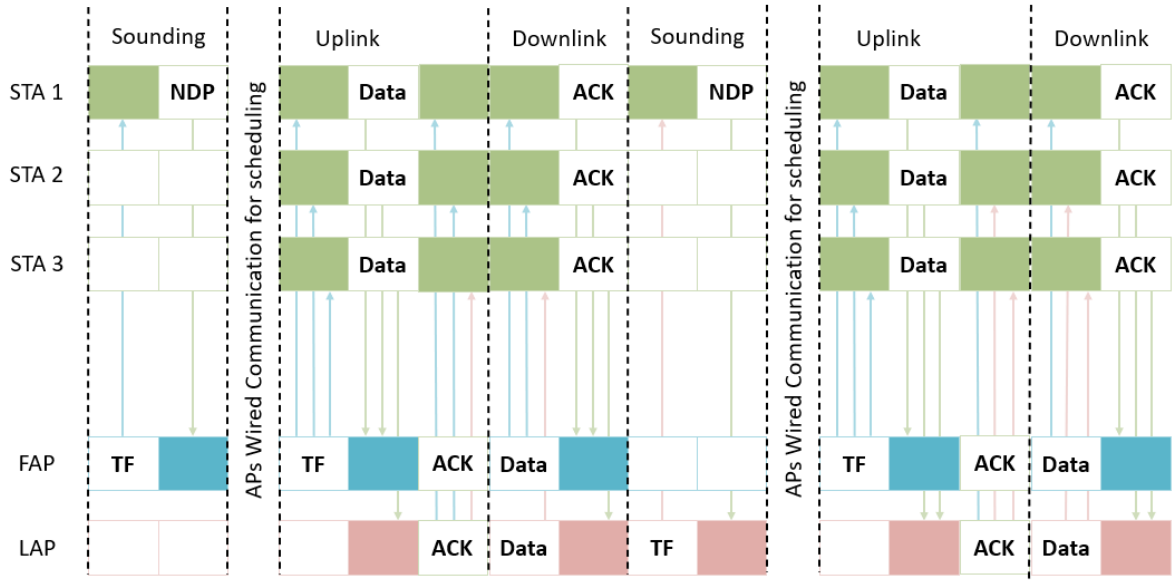

Figure 3. Two frame exchange cycles, Sounding-Scheduling-Data.

can reduce wireless interference and enhance the network's reliability.

B. Multi-AP Coordination

Multi-AP Coordination schemes are based on a Follower-Leader structure: one AP is selected as the Leader AP (LAP) and the remaining are established as Follower APs (FAPs). The LAP decides the coordination level of the network and the resource allocation based on the information gathered by itself and by the FAPs.

The LAP and FAPs must implement a low-latency backbone to exchange the control data. The backbone communication between APs could be wired or wireless depending on the deployment and implementation. If wireless, the constitution of the network would be first initiated by discovering beacons followed by information exchange about the status and characteristics of each AP for deciding which candidate would suit best as LAP. For this work we have assumed that such communication is wired and that there is no communication failures between APs.

A total of four techniques have been proposed for the IEEE 802.11be standard, which are briefly described as follows:

a) **Coordinated OFDMA (C-OFDMA):** The APs are coordinated to avoid possible overlapping between the RUs that they are using, which minimizes the interference between networks and enhances the PER. This technique is depicted in Figure 2.

b) **Coordinated Spatial Reuse (CSR):** Control the transmission power of the APs to reduce interference and allow simultaneous transmission.

c) **Coordinated Beamforming (CBF):** Allows simultaneous transmission with no interference by ensuring spatial nulls in the direction of the STAs outside the BSS.

d) **Joint Transmission:** Also known as Distributed MIMO allows the APs to perform joint data transmissions to the same STA by reusing the same time and frequency resources. Spatial diversity can be exploited to increase the probability of frame reception.

Of the four techniques, CSR involves very little complexity because it does not involve fast AP coordination, though its performance gain is limited because it does not perform any online coordination between APs and can only limit interference to some extent. On the other hand, CBF and JTx present a very high implementation complexity, require a nearly static scenario, and, in the case of JTx, tight synchronization between APs [20]. Finally, C-OFDMA presents a reasonable trade-off between implementation complexity and performance. C-OFDMA extends OFDMA from a single AP to multiple APs, which leads to efficient utilization of frequency resources across the network. Additionally, it can also enable the dynamic allocation of the spectrum among the APs [21]. That is, the available RUs can be assigned to each AP without any overlapping RUs.

C-OFDMA clearly limits the interference among devices of the same network and enables the implementation of smart scheduler strategies to enhance the network performance. Therefore, this paper is focused on C-OFDMA and will be addressed as Multi-AP Coordination further on. The scheduling techniques used over C-OFDMA can effectively enhance some performance targets. For instance, the scheduler strategy within the scope of WTSN could be focused on maximizing the probability of successfully delivering the data of every STA in the network and therefore reducing the network worst-case latency. Through the next section, we propose a scheduler algorithm and a set of sounding mechanisms that are focused on minimizing the PER of the wireless network.

III. SCHEDULING ALGORITHM AND SOUNDING MECHANISMS

This section first describes the scheduling proposals for allocating the users in the available frequency resources. The scheduling strategies are based on the knowledge of the Channel State Information (CSI) of each link between AP and STA. From this information, the scheduler must select which is the best communication resources combination for the

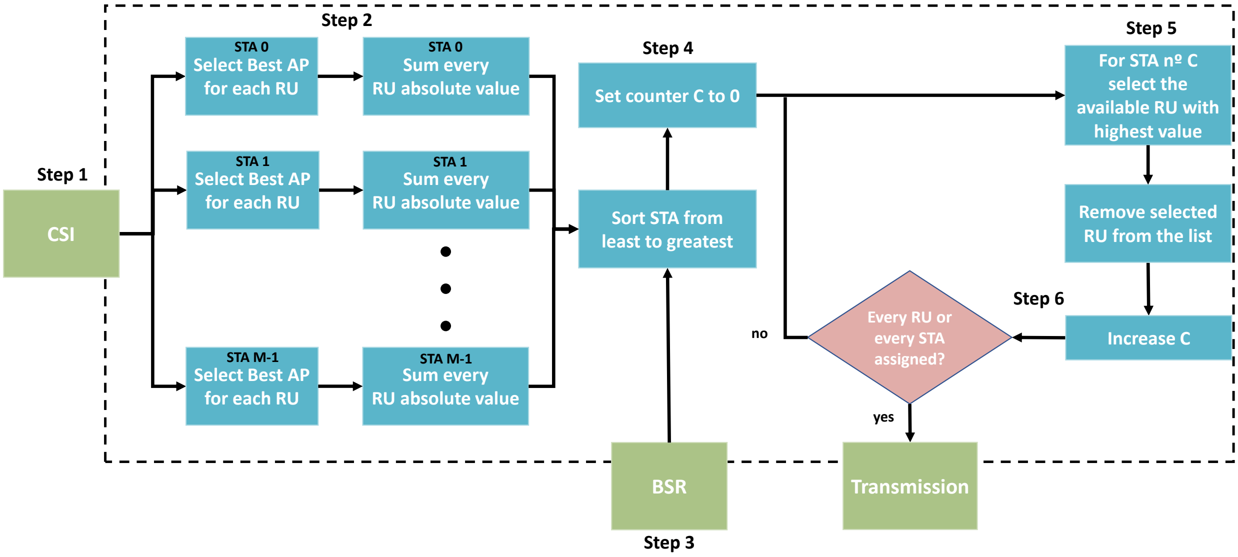

Figure 4. Scheduler Algorithm, assigns the frequency resources to the STAs by selecting the best RU combination.

whole network. That is, the combination that minimizes the overall PER in all the transmissions. Subsection III.A. presents the proposed scheduling algorithm for C-OFDMA. In addition, subsection III.B. presents the frame exchange used to obtain the CSI required by the scheduling algorithm.

A. C-OFDMA Scheduler Algorithm

The frame exchange proposed in this study comprises five phases as shown in Figure 3. These phases conform a communication cycle with duration T_{cycle} that periodically repeats. The communication cycle starts with a sounding phase (1), used by the APs to retrieve the CSI from the selected STAs. Then, the BSR exchange (2) allows the APs to know the amount of pending data that each STA needs to transmit. Based on the information gathered from (1) and (2), the LAP evaluates the situation (3) and decides the allocation of wireless resources used to transmit the data during the communication cycle. Finally, phases (4) and (5) perform the data exchange between APs and STAs.

For every communication cycle, the LAP will have to select the best RU combination possible that maximizes the probability of a successful transmission for every STA in the network. To do so, we propose a scheduler algorithm that bases the RUs allocation on the channel quality between STAs and APs for every link combination. The scheduler algorithm is depicted in Figure 4 and described as follows. Let us assume that the network comprises a total of N APs, M STAs, and a bandwidth B divided into K RUs.

- **Step 1**: The LAP Obtains/estimates the CSI of every RU between the STAs and APs provided by the sounding (a total of $N \cdot M \cdot K$ CSIs).
- **Step 2**: The algorithm sorts the STAs (STA_0 to STA_{M-1}) from worst channel quality to best channel quality. The channel quality can be defined in various ways. In this case, we have used the mean of the channel gain of the RUs/APs for each STA. This order dictates which STA is allocated first. Therefore, the worst STA on average would be able to obtain the best RU before the rest.
- **Step 3**: The STAs which BSR indicates that there is no data to be transmitted are discarded.
- **Step 4**: Set the STA counter (C) to zero.
- **Step 5**: Select the best RU for the STA_C to transmit their data according to the CSI metric described in step 3.
- **Step 6**: Once the RU for the STA_C to a given AP is selected, the RU is no longer eligible. Then, C is increased, and step 5 is repeated until no more RUs are available or all the STAs have been allocated. Note that if there are more STAs in the network than RUs available, the STAs with the best channel quality on average would not transmit in the current cycle. These STAs will be allocated in the next current cycle and will have an opportunity to transmit their data.

The scheduler attempts to maximize the probability of successfully deliver the information for every STA in the network. However, the scheduler lies on having good knowledge of the channel to perform the scheduling. The next subsections describe the mechanisms to obtain the information of the channels that serve as an input for the algorithm.

B. Channel sounding process

To select the best frequency-AP combination for the STAs transmission, knowledge about the CSI is required. There are two possible methods to obtain the CSI in IEEE 802.11: implicit and explicit feedback sounding. Implicit feedback sounding assumes that the physical channel is reciprocal. Therefore, an AP can measure the CSI between the AP and a STA just by receiving one frame. If the channel is reciprocal, the AP can safely assume that the measured CSI (STA to AP) is valid for the opposite direction (AP to STA). However, there might be some differences in the RF stages of the wireless devices which hurdle perfect reciprocity [22]. These differences may be critical, especially for some transmission techniques, such as beamforming and MIMO.

On the other hand, explicit feedback assumes that there is no perfect reciprocity. Therefore, if the AP wants the CSI from the link AP to STA, the AP first transmits a frame. Then, the STA measures the CSI from that frame. Finally, the STA transmits to the AP an IEEE 802.11 CSI report frame. This frame will carry a quantized representation of the CSI measured by the STA. As can be seen, explicit feedback presents a significant overhead, and it is only required in some situations such as large differences in the devices' RF stages and for MIMO transmissions [22]. Therefore, in the case of C-OFDMA, implicit feedback is a more suitable option since its precision is enough and it involves less complexity.

As depicted in Figure 3, each communication cycle is initiated by a TF from an AP. First, the LAP commands to one AP of the network (the LAP itself might be chosen) to transmit the TF to an STA. The STA receives the TF and responds with a Null Packet, which will be used by the AP to measure the CSI in the communication bandwidth. The selected AP will send the measured CSI to the LAP. Unfortunately, the LAP needs the CSI of every combination of APs/STAs ($M \cdot N$) to use the scheduler algorithm. Since the sounding of each link in every communication cycle generates significant overhead, the LAP can use virtual sounding. That is, instead of measuring the CSI of every link in every cycle, the APs may measure some links and interpolate the remaining CSIs from old measurements. IV.

C. Virtual Sounding

The best scheduling decisions come with perfect information about every single channel. However, this is hardly possible in practice, due to the excessive frame exchange needed for sounding all the possible links in a short period of time.

Since having perfect information for every channel at once is almost impossible, we propose three methods to virtually calculate the variations of the channels while estimating or sounding one of the links per transmission cycle. Note that in this work it is took for granted that every AP is always able to retrieve the CSI of the STA under measurement and therefore estimate the radio channel.

The simplest approach consists in keeping the last measured channel coefficient value of a link until the next sounding. If only one CSI measurement is done in a communication cycle, therefore the sounding refresh time of a specific link will be $T_{sounding} = N_{STA} * N_{AP} * T_{cycle}$. It is of utter importance for the coherence time of the channel to be higher than $T_{sounding}$ to be able to appropriately apply the scheduler algorithm.

The idea behind the next two methods is to gather the channel measurements in a fixed-size buffer with a First In First Out (FIFO) mechanism and use such coefficients to estimate the CSI in further transmissions without the need of sounding them. The first approach is based on a polynomial regression that adjusts to the variations of the measured CSIs gathered in a buffer. The size of the buffer and the grade of the polynomial might vary depending on the network. The next method resamples the input sequence at P times the original sample rate. Where P is the value that allows the output length of the signal to match the value of $T_{sounding}$ that indicates the number of samples before the conventional sounding is performed again. It applies a FIR Antialiasing Lowpass Filter to the input and compensates for the delay introduced by the filter.

Figure 5 depicts the evolution in one link of the channel gains for an example network comprised of 2 APs and 3 STAs. The dotted curve represents the real channel coefficients whereas the rest of the curves depict the predictive algorithms which, for this network size, must predict six straight channel gains prior update.

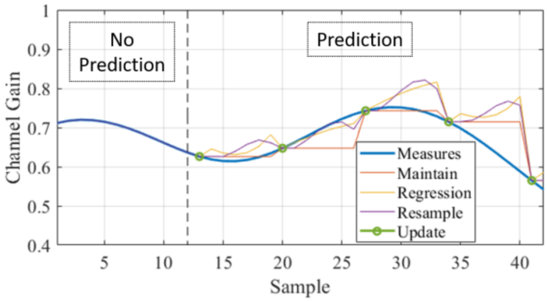

Figure 5. Sounding approaches over a link of a network comprised of 2 AP and 3 STA with a target speed of 2.5 km/h.

SIMULATION SCENARIO

This section presents the implementation details of the simulations carried out in Matlab to evaluate the proposed C-OFDMA scheduler algorithm and sounding mechanisms.

A. Wireless Channel Model

Matlab WLAN Toolbox has included the spatial channel models created by the ac task group (TGac) for different indoor and outdoor scenarios. From all the models in [23], the profile E propagation scenario is extracted from Indoor Large Offices/Warehouses, and it is meant for Indoor Hotspots with large rooms. We consider that profile E is the model that suits best for factory floors. In addition, we consider a RU bandwidth of 2 MHz, which can be considered as flat fading for profile E.

The coherence time of the wireless channel is the main limitation of the virtual sounding mechanism. The coherence time dictates the variation speed of the channel and therefore which is the maximum tolerable $T_{sounding}$. The coherence time is calculated as the inverse of the frequency doppler, which depends on the movement speed of the environment and the carrier frequency of the communication. is needed since it will constrict the size of the network due to the increase of the buffer refresh rate. Such time is related to the Doppler effect, and therefore, the speed of the wireless devices and environment.

The maximum doppler frequency f_d of the channel is calculated as follow.

$$f_d = f_c * \left(\frac{c+v}{c} - 1\right) \quad (1)$$

where f_c is the carrier frequency, c is the speed of light and v is the speed of the devices and environment [22].

There is more than one method to calculate the coherence time of a channel since its definition might vary depending on the application, for this study we consider that is the duration until the power of the signal autocorrelation ρ decays 3 dB [24].

$$\rho(\Delta t) = \frac{E\{h(t)h(t+\Delta t)^*\}}{E\{|h(t)|^2\}} \quad (2)$$

where $E\{\cdot\}$ is the expectation operator, $|\cdot|$ is the absolute value operator, *h(t)* is the impulse response of the channel, and

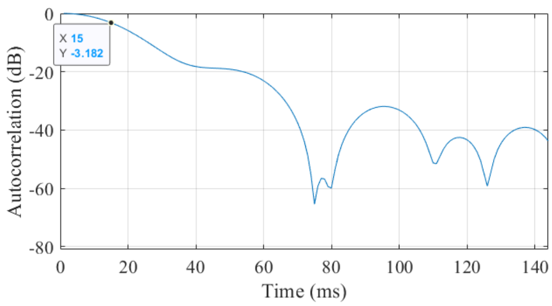

Figure 6. Autocorrelation of the signal in dB at 2.5 km/h.

Table 1. Coherence time of the channel for 5.25 GHz carrier frequency.

	Speed km/h							
	1	**2.5**	**4**	**5**	**6**	**7.5**	**9**	**10**
Coherence time (ms)	70	30	20	16	14	12	10	8

Δt is the coherence time at different thresholds. The Figure 6 shows the autocorrelation ρ for the selected wireless channel. For illustrative purposes, Table 1 collects the coherence times for different target speeds and a carrier frequency of 5.25 GHz.

B. Proposed Scenarios

In this subsection the different setups proposed for the simulations are defined, from all possible variables some will be fixed for every simulation and others will vary:

- Fixed parameters:
  - Channel bandwidth of 80 MHz.
  - Data packet size to 40 bytes.
  - Channel propagation model.
- Variable parameters:
  - Number of AP.
  - Number of STA.
  - Size of the buffer for virtual sounding.
  - Interpolation technique for virtual sounding (regression polynomial, resample, or maintain).
  - Doppler Effect.

All variable parameters are related to the performance of the virtual sounding mechanism. The larger the network the more cycles are needed to evaluate every link which will force the virtual sounding to work with outdated channel coefficients while the channel keeps varying. This becomes more critical if the coherence time of the channel is low which is related to the Doppler Effect and therefore the speed of the target. On the other hand, the size of the buffer and the degree of the polynomial determines the accuracy of the samples interpolated by the virtual sounding.

Both polynomial grade and buffer size parameters will be first studied in order to select the best combination possible for every proposed network. These networks could be divided into three different groups 1) Networks in which the buffer refresh rate is much lower than the coherence time of the channel, 2) Networks with similar buffer refresh rate and channel coherence time, and 3 Networks in which the buffer refresh rate surpasses the coherence time of the channel.

V. RESULTS

For the sake of comparison, we have established two benchmark approaches that will set the theoretical limits in terms of reliability. First, a random scheduler that allocates the users arbitrarily in the available RUs, a method that will presumably provide the worst possible results in terms of reliability. Second, we feed the C-OFDMA scheduler with perfect information about every channel.

A. Virtual Sounding Analysis

The virtual sounding has some input parameters that modify their performance and need to be determined for each scenario. In order to select such parameters, we first analyze the Mean Squared Error (MSE) of the algorithms regarding the measured channel coefficients. For each scenario we choose the configuration that provides the lower MSE. The polynomial regression and resampling techniques require some previous configurations that vary depending on the given scenario. For different network sizes we have calculated the MSE using from linear polynomials to grade 9 polynomials, a target speed of 2.5 km/h, and a $T_{cycle} = 2$ ms.

As shown in Table 2 the best polynomials for small networks are between grades 2 and 5, for bigger networks the best MSE is achieved with linear regression. Note that for bigger networks the coherence time is surpassed since the buffer refresh increases. This sets the MSE limit or threshold for the correct behavior of the prediction which is indicated by the cells highlighted in green.

Once the polynomial grade is chosen the next step is to set the buffer size. Small buffer sizes contain less information, but they are easier for the polynomial to adjust. Large buffer sizes on the other hand provide more information about the channel but might cause the polynomial to drift or diverge.

¡Error! No se encuentra el origen de la referencia. contains the MSE of different scenarios conformed by varying the buffer size, for each of the network proposals the best buffer length is chosen. Finally, we simulate all three techniques with different Doppler effects. For the polynomial and resample methods the configurations obtained in the previous Tables are used.

¡Error! No se encuentra el origen de la referencia. shows how the MSE deteriorates with the speed of the target where for 10 km/h no technique is able to provide an acceptable behavior, no matter the size of the network. As represented in Table 1 the coherence time of the channel at such speed is only 8 ms, being too low for the buffer refresh time to adapt to it. It is worth mentioning that such speed can be considered high, and it may not be the typical variation speed found in industrial environments. If the variation speed is larger than 10 km/h, some optimizations may be required (e.g., reducing the number of STAs or T_{cycle}).

Table 2. Mean Square Error at 2.5 km/h varying the Polynomial grade for the predict mode and the Network size.

		Network Size (AP x STA)							
		2x3	**2x4**	**2x5**	**2x6**	**2x7**	**2x8**	**2x12**	**2x15**
Polynomial	1	0.123	0.227	0.30	0.40	0.43	0.49	0.70	0.83
	2	**0.042**	0.092	0.17	0.26	0.35	0.42	0.79	1.04
	3	0.043	**0.074**	**0.12**	0.17	0.26	0.35	0.77	1.02
	4	0.051	0.080	**0.12**	**0.16**	0.22	0.30	0.71	0.93

	5	0.050	0.081	0.12	0.17	0.22	0.28	0.66	0.89
	6	0.052	0.085	0.12	0.17	**0.21**	0.28	0.65	0.89
	7	0.054	0.085	0.12	0.17	0.23	0.28	0.66	0.90
	8	0.055	0.086	0.12	0.18	0.23	0.30	0.64	0.92
	9	0.053	0.085	0.13	0.18	0.24	0.30	0.68	0.94

Table 3. Mean Square Error at 2.5 km/h varying the Network and buffer size.

			Network Size (AP x STA)				
			2x3	**2x4**	**2x5**	**2x6**	**2x7**
Buffer Size	**2**	Poly	**0.038**	**0.068**	**0.10**	**0.15**	**0.22**
		Resample	**0.038**	**0.069**	**0.10**	**0.15**	**0.22**
	3	Poly	0.053	0.090	0.12	0.17	**0.22**
		Resample	0.063	0.092	0.13	0.17	**0.22**
	4	Poly	0.039	0.077	0.11	0.16	**0.22**
		Resample	0.048	0.083	0.12	0.16	**0.22**
	5	Poly	0.044	0.073	0.11	0.17	**0.22**
		Resample	0.054	0.084	0.12	0.17	**0.22**

Table 3. Mean Square Error varying the speed and the Network size.

			Network Size				
			2x3	**2x4**	**2x5**	**2x6**	**2x7**
Speed km/h	**1**	Maintain	**0.0076**	**0.013**	**0.019**	**0.029**	**0.038**
		Poly	**0.0075**	**0.011**	**0.016**	**0.024**	0.046
		Resample	**0.0078**	**0.011**	**0.017**	**0.024**	0.046
	2.5	Maintain	0.049	0.080	0.12	0.17	**0.22**
		Poly	**0.038**	**0.068**	**0.10**	**0.15**	**0.22**
		Resample	**0.037**	**0.069**	**0.10**	**0.15**	**0.22**
	4	Maintain	0.11	**0.19**	**0.28**	0.38	0.49
		Poly	**0.10**	**0.18**	0.30	0.42	0.60
		Resample	**0.10**	**0.18**	0.30	0.42	0.57
	5	Maintain	**0.17**	**0.29**	0.40	0.54	0.66
		Poly	**0.17**	0.30	0.46	0.64	0.85
		Resample	**0.17**	0.30	0.46	0.64	0.81
	10	Maintain	0.54	0.78	0.94	1.09	1.18
		Poly	0.67	0.98	1.16	1.34	1.51
		Resample	0.66	0.97	1.15	1.34	1.45

B. Network Performance

The next step is to analyze the performance of the proposed techniques with a full model comprised of the network, the scheduler, and the modems. To compare each of the algorithms along with the benchmark indicators, we have extracted the PER simulating 10^5 packets per average SNR point from 0 dB to 20 dB in steps of 1 dB and we have set $T_{cycle} = 2$ ms.

Two curves set the worse and the best case for each of the scenarios. The Random curve in blue is obtained by applying no smart scheduler, assigning the channels arbitrarily. Whereas the Full Sounding curve in red is calculated by using the intelligent scheduler and full knowledge of the quality of every channel in every cycle. Note that the implementation of the latter is close to impossible and is used as a theoretical limit. This is because, in order to implement the Full Sounding

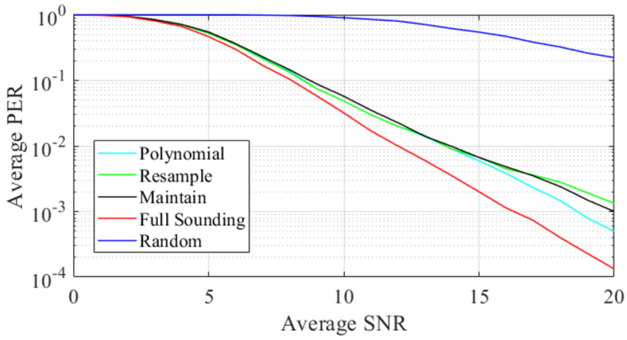

Figure 7. PER for a network of 2 AP, 3 STA and 2.5 km/h $T_{sounding} = 12$ ms.

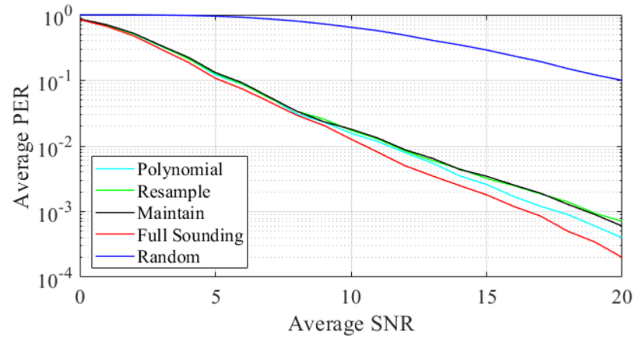

Figure 8. PER for a network of 2 AP, 7 STA and 1 km/h, $T_{sounding} = 28$ ms.

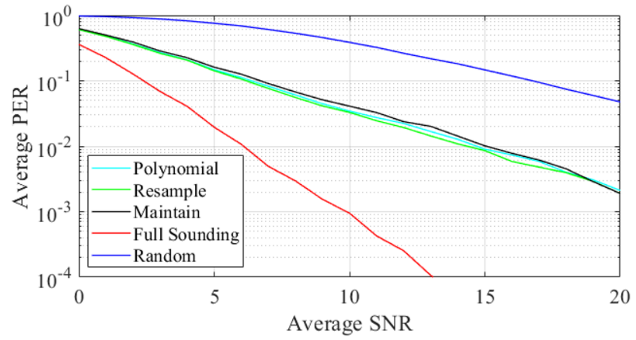

Figure 9. PER for a network of 3 AP, 15 STA and 1 km/h, $T_{sounding} = 90$ ms.

method, every link combination between AP/STAs must be sounded in every communication cycle.

As depicted in Fig. 7 and Fig. 8 when the refresh rate of the buffer ($T_{sounding}$) is lower than the coherence time of the channel, the performance of the techniques is almost identical to the Full Sounding approach. When $T_{sounding}$ gets closer or surpasses the coherence time, the performance starts to deteriorate. This is clearly shown in Fig. 9, with a $T_{sounding} =$ 90 ms and a channel coherence time of 70 ms. The CSI of a STA is precise after the corresponding sounding and for several communication cycles, though it starts to deteriorate when the measured CSI gets older. To overcome this issue, each communication cycle may need two or more CSI measurements. More CSI measurements will significantly reduce $T_{sounding}$ and improve the CSI estimation.

In addition to this, it is clear from the results that increasing the number of APs also enhances the achievable PER in the network. The number of available links for each STA increases, which translates into better probability of founding a good RU to transmit their data.

Conclusions

In this paper, we have presented a detailed evaluation of one of the most promising techniques proposed for IEEE 802.11be to enhance the PER and latency for industrial wireless communications: the C-OFDMA Multi-AP Coordination. The analysis presented shows that C-OFDMA could have potential gains in terms of PER, thus reducing latency (fewer retransmissions required). However, C-OFDMA's main limitation comes from the need of accurate and fresh channel information between the APs and STAs to dynamically adjust the network's scheduling. Since the update of the channel information causes a large overhead in the network, the paper shows a set of techniques to reduce the channel sounding rate.

Our numerical simulation results highlight that C-OFDMA significantly improves the PER of the communications, though the performance gains significantly depend on the availability of accurate channel information, which in turn depends on the channel variation speed. Therefore, C-OFDMA presents significant gains for low-varying conditions and small-sized networks, whereas the performance gains are limited if such conditions are not met.

In future research, we plan to extend this analysis to further improve our proposed scheduling algorithms and combine Multi-AP Coordination with other techniques proposed for 802.11 such as Multi-Link Operation.

References

[1] "Time-sensitive networking (TSN) task group." 2021, [Online]. Available: https://1.ieee802.org/tsn/.

[2] B. Chen, J. Wan, L. Shu, P. Li, M. Mukherjee, and B. Yin, "Smart Factory of Industry 4.0: Key Technologies, Application Case, and Challenges," IEEE Access, vol. 6, pp. 6505–6519, 2017, doi: 10.1109/ACCESS.2017.2783682.

[3] T. S. A. Grau, M. Indri, L. L. Bello, "Industrial robotics in factory automation: From the early stage to the Internet of Things," ECON 2017 - 43rd Annu. Conf. IEEE Ind. Electron. Soc., pp. 6159–6164, 2017, doi: 10.1109/IECON.2017.8217070.

[4] W. Rong, G. T. Vanan, and M. Phillips, "The internet of things (IoT) and transformation of the smart factory," Proc. - 2016 Int. Electron. Symp. IES 2016, pp. 399–402, 2017, doi: 10.1109/ELECSYM.2016.7861039.

[5] F. Tramarin, A. K. Mok, and S. Han, "Real-Time and Reliable Industrial Control over Wireless LANs: Algorithms, Protocols, and Future Directions," Proc. IEEE, vol. 107, no. 6, pp. 1027–1052, 2019, doi: 10.1109/JPROC.2019.2913450.

[6] M. Luvisotto, Z. Pang, and D. Dzung, "High-Performance Wireless Networks for Industrial Control Applications: New Targets and Feasibility," Proc. IEEE, vol. 107, no. 6, pp. 1074–1093, 2019, doi: 10.1109/JPROC.2019.2898993.

[7] "IEEE P802.11ax D6.0. Draft Standard for Information technology - Telecommunications and information exchange between systems Local and metropolitan area networks - Specific requirements." .

[8] "3GPP; Technical Specification Group Services and System Aspects; System architecture for the 5G System (5GS) Stage 2 (Release 16) 3GPPTS 23.501 V16.4.0." .

[9] D. Cavalcanti, J. Perez-Ramirez, M. M. Rashid, J. Fang, M. Galeev, and K. B. Stanton, "Extending Accurate Time Distribution and Timeliness Capabilities over the Air to Enable Future Wireless Industrial Automation Systems," Proc. IEEE, vol. 107, no. 6, pp. 1132–1152, 2019, doi: 10.1109/JPROC.2019.2903414.

[10] E. Khorov, A. Kiryanov, A. Lyakhov, and G. Bianchi, "A tutorial on IEEE 802.11ax high efficiency WLANs," IEEE Commun. Surv. Tutorials, vol. 21, no. 1, pp. 197–216, 2019, doi: 10.1109/COMST.2018.2871099.

[11] G. Lacalle, I. Val, O. Seijo, M. Mendicute, D. Cavalcanti, and J. Perez-Ramirez, "Analysis of Latency and Reliability Improvement with Multi-Link Operation over 802.11," pp. 1–7, 2021, doi: 10.1109/indin45523.2021.9557495.

[12] M. Yang, B. Li, Z. Yan, and Y. Yan, "AP Coordination and Full-duplex enabled Multi-band Operation for the Next Generation WLAN: IEEE 802.11be (EHT)," 2019 11th Int. Conf. Wirel. Commun. Signal Process. WCSP 2019, 2019, doi: 10.1109/WCSP.2019.8928021.

[13] D. Bankov, A. Didenko, E. Khorov, V. Loginov, and A. Lyakhov, "IEEE 802.11ax uplink scheduler to minimize delay: A classic problem with new constraints," IEEE Int. Symp. Pers. Indoor Mob. Radio Commun. PIMRC, vol. 2017-October, pp. 1–5, 2018, doi: 10.1109/PIMRC.2017.8292382.

[14] Y. G. Dandan Liang, Ming Gan, Guogang Huang, Yu Jian, "One Channel Information Feedback Method for Multi-AP Coordination." 2019, [Online]. Available: https://mentor.ieee.org/802.11/dcn/19/11-19-1573-00-00be.

[15] M. Ge and D. M. Blough, "High throughput and fair scheduling for Multi-AP Multiuser MIMO in dense wireless networks," IEEE/ACM Trans. Netw., vol. 26, no. 5, pp. 2414–2427, 2018, doi: 10.1109/TNET.2018.2867582.

[16] G. Z. Islam and M. A. Kashem, "Efficient resource allocation in the IEEE 802.11ax network leveraging OFDMA technology," J. King Saud Univ. - Comput. Inf. Sci., no. xxxx, 2020, doi: 10.1016/j.jksuci.2020.10.019.

[17] W. Ahn, "Novel multi-AP coordinated transmission scheme for 7th generation WLAN 802.11be," Entropy, vol. 22, no. 12. pp. 1–19, 2020.

[19] C. Deng et al., "IEEE 802.11be-Wi-Fi 7: New Challenges and Opportunities," arXiv, pp. 1–30, 2020, doi: 10.1109/comst.2020.3012715.

[20] S. R. Xiaogang Chen, Qinghua Li, Feng Jiang, Ziv Avital, Laurent Cariou, Kenney Thomas, "Discussions of Multi-AP JT," 2019.

[21] J. C. Sungjin Park, Jeongki Kim, Suhwook Kim, Insun Jang, Taewon Song, Namyeong Kim, "Considerations on Coordinated OFDMA," 2020.

[22] H. Lou, M. Ghosh, P. Xia, and R. Olesen, "A comparison of implicit and explicit channel feedback methods for MU-MIMO WLAN systems," IEEE Int. Symp. Pers. Indoor Mob. Radio Commun. PIMRC, pp. 419–424, 2013, doi: 10.1109/PIMRC.2013.6666172.

[23] V. J. R. Vinko Erceg, Laurent Schumacher, Persefoni Kyritsi, Andreas Molisch, Daniel S. Baum, Alexei Y. Gorokhov, Claude Oestges, Qinghua Li, Kai Yu, Nir Tal, Bas Dijkstra, Adityakiran Jagannatham, Colin Lanzl, "IEEE P802.11 Wireless LANs, TGn Channel Model." [Online]. Available: doc.: IEEE 802.11-03/940r4.

[24] M. S. John G. Proakis, Communication Systems Engineering(2nd Edition). 2002.